NeuroImage: Clinical 7 (2015) 721–731

Contents lists available at ScienceDirect

NeuroImage: Clinical

journal homepage: www.elsevier.com/locate/ynicl

Diffuse alterations in grey and white matter associated with cognitive impairment in Shwachman–Diamond syndrome: Evidence from a multimodal approach

Sandra Perobelli [a,*], Franco Alessandrini [b], Giada Zoccatelli [b], Elena Nicolis [c], Alberto Beltramello [b], Baroukh M. Assael [a], Marco Cipolli [a]

[a] Cystic Fibrosis Centre, Azienda Ospedaliera Universitaria, Piazzale Stefani, 1-37126 Verona, Italy
[b] Neuroradiology Department, Azienda Ospedaliera Universitaria, Piazzale Stefani, 1-37126 Verona, Italy
[c] Laboratory of Molecular Pathology, Laboratory of Clinical Chemistry and Haematology, Azienda Ospedaliera Universitaria, Piazzale Stefani, 1-37126 Verona, Italy

ARTICLE INFO

Article history:
Received 22 April 2014
Received in revised form 5 February 2015
Accepted 22 February 2015
Available online 27 February 2015

Keywords:
Shwachman–Diamond syndrome
Cognitive impairment
Structural MRI
Functional MRI
Diffusion tensor imaging
Tract-based Spatial Statistics

ABSTRACT

Shwachman–Diamond syndrome is a rare recessive genetic disease caused by mutations in SBDS gene, at chromosome 7q11. Phenotypically, the syndrome is characterized by exocrine pancreatic insufficiency, bone marrow dysfunction, skeletal dysplasia and variable cognitive impairments. Structural brain abnormalities (smaller head circumference and decreased brain volume) have also been reported. No correlation studies between brain abnormalities and neuropsychological features have yet been performed. In this study we investigate neuroanatomical findings, neurofunctional pathways and cognitive functioning of Shwachman–Diamond syndrome subjects compared with healthy controls. To be eligible for inclusion, participants were required to have known SBDS mutations on both alleles, no history of cranial trauma or any standard contraindication to magnetic resonance imaging. Appropriate tests were used to assess cognitive functions. The static images were acquired on a 3 × 0 T magnetic resonance scanner and blood oxygen level-dependent functional magnetic resonance imaging data were collected both during the execution of the Stroop task and at rest. Diffusion tensor imaging was used to assess brain white matter. The Tract-based Spatial Statistics package and probabilistic tractography were used to characterize white matter pathways.

Nine participants (5 males), half of all the subjects aged 9–19 years included in the Italian Shwachman–Diamond Syndrome Registry, were evaluated and compared with nine healthy subjects, matched for sex and age. The patients performed less well than norms and controls on cognitive tasks ($p = 0.0002$).

Overall, cortical thickness was greater in the patients, both in the left (+10%) and in the right (+15%) hemisphere, significantly differently increased in the temporal (left and right, $p = 0.04$), and right parietal ($p = 0.03$) lobes and in Brodmann area 44 ($p = 0.04$) of the right frontal lobe. The greatest increases were observed in the left limbic-anterior cingulate cortex (≥43%, $p < 0.0004$). Only in Broca's area in the left hemisphere did the patients show a thinner cortical thickness than that of controls ($p = 0.01$).

Diffusion tensor imaging showed large, significant difference increases in both fractional anisotropy (+37%, $p < 0.0001$) and mean diffusivity (+35%, $p < 0.005$); the Tract-based Spatial Statistics analysis identified six abnormal clusters of white matter fibres in the fronto-callosal, right fronto-external capsulae, left fronto-parietal, right pontine, temporo-mesial and left anterior–medial–temporal regions. Brain areas activated during the Stroop task and those active during the resting state, are different, fewer and smaller in patients and correlate with worse performance ($p = 0.002$).

Cognitive impairment in Shwachman–Diamond syndrome subjects is associated with diffuse brain anomalies in the grey matter (verbal skills with BA44 and BA20 in the right hemisphere; perceptual skills with BA5, 37, 20, 21, 42 in the left hemisphere) and white matter connectivity (verbal skills with alterations in the fronto-occipital fasciculus and with the inferior-longitudinal fasciculus; perceptual skills with the arcuate fasciculus, limbic and

Abbreviations: BOLD, blood oxygen level-dependent; BA, Brodmann area; CTA, cortical thickness analysis; DTI, diffusion tensor imaging; EPI, Echo-planar Imaging; FA, fractional anisotropy; FDT, Diffusion Toolbox; GLM, General Linear Model; ICA, independent component analysis; MD, mean diffusivity; PD, parallel diffusivity; PT, probabilistic tractography; RD, radial diffusivity; rs-fMRI, resting state fMRI; SDS, Shwachman–Diamond syndrome; TBSS, Tract-based Spatial Statistics.

* Corresponding author at: Cystic Fibrosis Centre, Azienda Ospedaliera Universitaria Integrata, Piazzale Stefani, 1-37126 Verona, Italy. Tel.: +39 0458122286.
E-mail address: sandra.perobelli@ospedaleuniverona.it (S. Perobelli).

http://dx.doi.org/10.1016/j.nicl.2015.02.014

ponto-cerebellar fasciculus; memory skills with the arcuate fasciculus; executive functions with the anterior cingulated and arcuate fasciculus).

1. Introduction

Shwachman–Diamond syndrome (SDS) (Shwachman et al., 1964) is a rare autosomal recessive disorder resulting from mutations in the SBDS gene on chromosome 7q11 (Boocock et al., 2003). The SBDS gene is highly expressed in rapidly proliferating tissues, but it was found to be expressed in all embryonic stages and most adult tissues, including in the brain (Zhang et al., 2006). Phenotypically, SDS is principally characterized by exocrine pancreatic insufficiency, bone marrow dysfunction and skeletal dysplasia (Cipolli, 2001). In early clinical descriptions of SDS (Bodian et al., 1964; Shwachman et al., 1964), contradictory data on psychomotor development were reported. Subsequently, three studies compared cognitive functioning in SDS children with healthy siblings and/or children with other chronic diseases, such as cystic fibrosis. Cognitive impairment has been noted in the majority of these patients, albeit with intragroup variability (Kent et al., 1990; Kerr et al., 2010; Perobelli et al., 2012); this has a serious impact on quality of life, limiting independence and socialization (Perobelli et al., 2012). With regard to aetiology, cognitive impairment was clearly characterized as primary, being independent of the family environment, malnutrition or suffering from a chronic illness (Kent et al., 1990; Kerr et al., 2010). The SBDS gene is expressed in all mammalian tissues, but little is known on imaging features or the histopathology of the brain. Two SDS subjects, a neonate with delayed myelination on MRI and an infant with agenesis of the corpus callosum on a CT scan, were described (Kamoda et al., 2005; Todorovic-Guild et al., 2006). More recently, two neuroimaging studies reported findings of SDS patients compared with sex-/age-matched healthy controls. A structural MRI study (Toiviainen-Salo et al., 2008) in nine patients with a wide age range (7–37 years: one child, three adolescents, five adults) reported decreased global brain volume, affecting both grey matter and white matter. In another study (Booij et al., 2013), structural MRI and single photon emission computed tomography in six SDS patients (12–26 years: two adolescents, four young adults) demonstrated smaller brain volumes, particularly posteriorly and caudally, and a dysregulated dopaminergic system. Neither of these studies performed cognitive evaluations. At present we do not have comprehensive studies that have considered and correlated neuroanatomical findings and neuro-cognitive performance to define the neuro-psychological phenotype of Shwachman–Diamond syndrome.

The growing consensus is that cognition is the result of the dynamic interaction of distributed brain areas linked within large-scale networks and connected by white matter tracts, rather than single cortical areas (Catani and ffytche, 2005; Catani and Mesulam, 2008; Ross, 2010; Bartolomeo, 2011). In a review of 37 studies, Jung and Haier (2007) developed a model (Parieto-Frontal Integration Theory) by which "variations in a distributed network predict individual differences found on intelligence and reasoning tasks …. White matter regions (i.e. arcuate fasciculus) are also implicated". Neuroimaging is a non-invasive technology that allows "in vivo" explorations of the brain structure and functioning and the brain development/maturation in typically and abnormally developing children. Characteristics of the grey and white matter are considered important determinants of interindividual differences in cognition (Luders et al., 2009). Cortical thickness (Catani, 2006; Lu et al., 2009; Tamnes et al., 2010; Goh et al., 2011), diffusion tensor imaging (DTI) measures (Smith et al., 2006; Chanraud et al., 2010; Freilich and Gaillard, 2010; Govindan et al., 2010a; Schmithorst and Yuan, 2010; Hegarty et al., 2012), Tract-based Spatial Statistics (TBSS) (Smith et al., 2006; Govindan et al., 2010b) and blood-oxygen-level-dependent (BOLD) signals (Freilich and Gaillard, 2010; Vlooswijk et al., 2010) are used as good parameters of grey matter maturation, microstructure integrity of white matter and brain activity respectively.

In the present study we adopted a multi-modal approach including general and specific neurocognitive tests, structural MRI, diffusion tensor imaging and tract based spatial statistics. We also used functional MRI to investigate brain activation and performance during an attentional colour–word task (Stroop test) (McLeod, 1991) and to detect the areas still active when the brain is "at rest" (the so called "default mode network"). The goal of our study was to describe and compare characteristic neuroanatomical findings, neurofunctional pathways and cognitive performance in an SDS group matched to healthy subjects.

We hypothesized that the cerebral areas mostly responsible for cognitive impairment (Catani, 2006; Jung and Haier, 2007; Sowell et al., 2008; Leech and Sharp, 2013) may be identified in the prefrontal, parietal and occipital cortices, and that impaired connectivity between the posterior and frontal areas may be found in SDS subjects.

2. Materials and methods

2.1. Participants

Ten individuals with SDS, aged 9–19 years, responded to the SDS Association's public invitation to participate in the study. These patients, accounting for half of all the subjects for this age group in the Italian SDS Registry, were included only if they carried one of the known SBDS mutations on both alleles. Nine healthy subjects, matched for gender and age, also participated in the study. The exclusion criteria were, for both groups: previous history of cranial trauma with loss of consciousness, or any of the standard contraindications to MRI. In order to avoid sedation, patients were only included if they were more than 8-year-old.

All subjects were fully informed about the study during personal discussions, both alone and with their parents. Explanations included an audio–visual session on the MRI procedure presented by a clinical psychologist, after which one child declined to proceed.

None of the subjects were affected by neuropsychiatric syndromes or were taking neuropsychiatric medication.

2.2. Assessment of cognitive performance and behaviour

All subjects underwent cognitive testing, designed to assess general and specific cognitive functions. We employed: a) the full Wechsler Intelligence Scale according to each patient's age (normal values 100 ± 15) (Wechsler D., 1981; Wechsler D., 1991). The following parameters were calculated: Full Scale Intelligence Quotient (FSIQ), Verbal IQ (VIQ), Performance IQ (PIQ), Verbal Comprehension, Perceptual Organization, Freedom From Distractibility and Processing Speed. The sub-test scores (normal values 10 ± 3) were also calculated; b) the Beery–Buktenica Developmental Test of Visual–Motor Integration (normal values 10 ± 3), plus the two supplementary Visual and Motor Tests, were administered to assess potential deficits in visual perception or in motor coordination or in their integration (Beery K.E. and Buktenica N.A., 1997); c) the Test of Memory and Learning was used with all its components, including Verbal, Non-verbal, Composite Memory and Delayed Recall, in order to identify subjects with disturbed retention of information (Reynolds and Bigler, 1994); d) the Wisconsin Card Sorting Test was administered as a measure of executive function (Heaton R.K. et al., 1981).

The tests were administered and scored by a senior clinical psychologist, experienced in paediatric psychometric assessment. Parents

provided information on the children's medical history and completed the Child Behavior Checklist (Achenbach, 1991) for the assessment of the child's social competence, emotional state and behaviour. The battery of tests was split into two parts, to be administered on two consecutive days, in order to avoid excessive fatigue and consequent bias when assessing intellectual functions. The order of testing was the same for all subjects.

2.3. Image acquisition and processing

All subjects underwent a head MRI. Images were acquired with a 3.0 T Siemens scanner (Siemens Allegra, Erlangen, Germany), using a standard head-coil. Foam pads and headphones were used to reduce head motion and scanner noise. Acquisition, analysis and processing of MRI images are detailed in the SI text. Briefly, the procedure included the steps detailed below:

a High resolution morphological 3D T1 weighted images (MPRAGE, TR = 1840 ms; TE = 2.83 ms; matrix = 256 × 256; slices = 160; slice thickness = 1 × 1 × 1 mm) were acquired with the Brain Voyager QX software (Brain Innovation, Maastricht, The Netherlands, http://www.brainvoyager.com) for cortical thickness analysis (CTA). This allows measurement of individually segmented cortical hemispheres and calculation of individual and group thickness values within any region of interest and Brodmann areas (BAs) (Brodmann, 1909). The cortical thickness measurements were analysed following the Laplace method (Jones, 2000). For each subject, the high resolution T1 image was routinely examined by a trained neuroradiologist for any significant structural anomalies:

b Blood oxygen level-dependent (BOLD) fMRI data were collected by using an Echo-planar Imaging (EPI) sequence, with axial slices parallel to the antero-posterior commissure (EPI TR = 2500 ms; TE = 30 ms; matrix = 64 × 64; slice = 36; slice thickness = 3.2 mm; 130 measurements). To investigate the differences in the pattern of activation of the neural circuits, a word-colour attentional Stroop task was used (Mc Leod, 1991). Resting state fMRI (rs-fMRI, EPI TR = 2610 ms; TE = 30 ms; matrix = 64 × 64; slice = 36; slice thickness = 3 mm; 200 measurements) was used to evaluate regional interactions when the subject was not performing an explicit task. This approach reflects structural connectivity within the default mode network, a set of brain regions – including the medial prefrontal cortex, medial temporal lobes and posterior cingulate cortex/retrosplenial cortex – implicated in episodic memory processing.

c Diffusion tensor imaging (DTI) was acquired in 30 directions, using values of B = 0 (B0) and B = 700 s/mm^2 (TR = 9000 ms; TE = 87 ms; matrix = 128 × 128; slices = 60; slice thickness = 1.9 × 1.9 × 1.9 mm) for an indication of the microstructure of white matter.

DTI is sensitive to the direction and extent of the diffusion of water in the brain, which is hindered by myelin sheaths and cell membranes and influenced by the level of myelination and axonal density. This diffusion is typically quantified by two derived measures: a) fractional anisotropy (FA), an index of the directionality of diffusion in each voxel, which reflects axonal diameter, axonal density and fibre tract complexity; b) mean diffusivity (MD), representing apparent mobility of water which reflects cellular density and extracellular volume and relates to the volume fraction of the interstitial space. Parallel diffusivity (PD) and radial diffusivity (RD) were also derived, as more specific sources of additional information concerning potential cellular impairment and spatial orientation of fibres. The total MRI examination time was 40 min.

2.4. Statistical analysis

Demographic and clinical data were expressed as mean values (SD) and median (range) for continuous variables, and as numbers and frequencies for categorical variables. Comparison between the cases and controls was done with the Mann–Whitney test (for cognitive tests, Stroop test, cortical thickness, FA and MD); the Spearman rank-correlation was calculated between cognitive performance and cortical thickness/white matter clusters. For all the analyses, an a priori decided significance level of $p < 0.05$ corrected (Bonferroni and FDR) was considered to be statistically significant. Spatial pre-processing and statistical inference testing of fMRI and rs-fMRI data were carried out using the software package Brain Voyager QX version 2.4 (Brain Innovation, Maastricht, The Netherlands, http://www.brainvoyager.com). Analysis was performed using the General Linear Model (GLM) for serially auto-correlated observations (Friston et al., 1994). The fMRI and rs-fMRI maps were submitted to a one-way repeated-measures ANOVA, to identify the regions of interest showing a main effect of condition. Predictors were compared, in each task on which the two groups differed significantly ($p < 0.05$, false discovery rate), to threshold statistical maps. In order to protect against false positives due to multiple comparisons, a contiguity threshold (minimum spatial extent) of 10 voxels was employed. Resting-state functional connectivity was calculated by independent component analysis (ICA) (Hyvarinen and Oja, 2000).

DTI images were statistically compared for regional differences using the Diffusion Toolbox (FDT) and the Tract-based Spatial Statistics (TBSS) package from FMRIB's Software Library (FSL, http://www.fmrib.ox.ac.uk/fsl/). The set of mean images for each subject was used to construct the diffusion tensor and to create maps of FA, RD, PD and MD, using DTIFIT from FSL. The TBSS method was used to minimize the potential misalignment problems of other voxel-based whole-brain analysis methods, by determining a white-matter "skeleton" restricted to the centre of the major white matter tracts, and mapping FA and MD values from each individual directly onto this standard skeleton for group comparison. A region of interest mask was manually generated for each of the significant clusters identified in the TBSS analysis. This was done by including only the voxels that showed a significant difference in FA (p corrected < 0.05).

To further characterize the origins and pathways of the white matter tracts in which abnormalities in FA were found, the probabilistic tractography (PT) method within the FSL software was used. Thus we obtained probabilistic connectivity maps representing the most likely paths extending from the clusters with abnormal FA. The cortical origins and endpoints of these connectivity paths were reported, based on an anatomical labelling template.

Statistical analysis was done with SAS, version 9.2 (SAS Institute Inc., Cary, NC, US).

This study was approved by the Ethics Committee of the Azienda Ospedaliera Universitaria di Verona.

3. Results

3.1. Participant characteristics, cognitive performance and behaviour

Demographic information and neurocognitive test scores are reported in Table 1, where SBDS mutations are also reported. Verbal and performance intelligence scores, as well as total score, were significantly lower in SDS patients, compared both to controls and to normal values. Overall, intellectual reasoning abilities of SDS patients ranged from severely impaired (score: 65) to normal (score: 97), with four SDS subjects showing scores below 1 SD (range 65–84; 1st–10th percentiles).

On visual–motor integration tasks, there were no significant differences.

All scores of verbal and non-verbal memory parameters were significantly lower in SDS patients.

On the executive function test (Wisconsin Card Sorting Test) eight SDS subjects did more perseverative errors (17% vs. 7%; $p = 0.05$, n.s.); one SDS child was not able to conclude the test.

Table 1
Demographic and clinical characteristics and cognitive performance of patients with Shwachman–Diamond syndrome (SDS) and healthy controls.

	SDS (n = 9)	Controls (n = 9)
Gender (M/F)	5/4	5/4
Age (mean ± SD and range)	13.5 ± 3.1 (9–19)	13.7 ± 3.2 (10–18)
Schooling mainstream	9 (2 with help)	9
Parents' attained grade		
Elementary/middle school	5	4
Junior high school	7	5
High school	4	5
College/university	2	4
SBDS mutations		
258+2T>C/183–184TA>CT	5	
258+2T>C/258+2T>C	2	
258+2T>C/352A>G	1	
258+2T>C/183–184TA>CT+258+2T>C	1	

Test	Median (range)	Median (range)	
Wechsler Scale			
FSIQ	87 (65–97)	119 (92–139)	0.0002
VIQ	82 (71–103)	119 (95–145)	0.0002
PIQ	84 (65–117)	114 (85–123)	0.002
Index scores			
Verbal Comprehension	84 (74–106)	119 (97–128)	0.0005
Perceptual Organization	85 (69–105)	107 (83–128)	0.004
Freedom From Distractibility	88 (66–103)	115 (97–130)	0.0002
Processing Speed	85 (68–112)	97 (91–112)	0.12
Subtests			
Information	7 (4–12)	12 (7–17)	0.01
Similarities	8 (7–11)	12 (9–15)	0.0008
Arithmetic	7 (5–10)	13 (7–14)	0.001
Vocabulary	9 (3–12)	14 (8–17)	0.001
Comprehension	6 (1–11)	13 (9–16)	0.001
Digit span	8 (3–12)	14 (9–17)	0.0003
Picture completion	8 (5–14)	11 (8–14)	0.06
Coding	6 (3–11)	9 (7–12)	0.12
Picture arrangements	7 (4–11)	11 (8–15)	0.007
Block design	7 (2–12)	11 (6–16)	0.02
Object assembly	9 (6–11)	11 (7–14)	0.06
Symbol search	10 (6–14)	10 (9–13)	0.34
Mazes	9 (5–15)	10 (7–12)	0.31
VMI			
Visual–motor integration	8 (6–13)	9 (6–16)	0.38
Visual	9 (4–13)	10 (7–14)	0.62
Motor	8 (5–12)	11 (7–14)	0.12
WCST			
% perseverative errors	17 (3–38)[a]	8 (0–17)	0.11
TOMAL — centile (range)			
Verbal memory	49 (23–87)	84 (32–97)	0.02
Non–verbal memory	26.5 (5–70)	79 (23–99)	0.002
Composite memory	35 (19–82)	82 (27–99)	0.007
Verbal delayed recall	61 (16–84)	84 (55–91)	0.05
CBCL (T scores)			
Activities[b]	33 (25–55)	46 (33–55)	0.04
Socialization[b]	42.5 (33–54)	55 (42–55)	0.009
School[b]	43.5 (26–51)	52 (45–54)	0.003
Total competencies[b]	33.5 (25–41)	53 (35–80)	0.001
Internalizing problems[c]	51.5 (46–61)	57 (49–66)	0.05
Externalizing problems[c]	49 (38–57)	46 (43–69)	0.61
Total problems[c]	54 (43–59)	50 (45–66)	0.69

FSIQ = full scale intelligence quotient; VIQ = verbal intelligence quotient; PIQ = perceptual intelligence quotient; VMI = visual–motor integration; WCST = Wisconsin card sort test; TOMAL = Test of Memory and Learning; CBCL = Child Behaviour Checklist.
[a] One SDS patient was not able to conclude the test, so the result was calculated on the scores of 8 SDS subjects.
[b] Normal values: T score > 35.
[c] Normal values: T score < 60.

In the Child Behaviour Checklist (Table 1), patients with SDS showed deterioration in both school activities and socialization, without significant emotional/behavioural problems.

3.2. Cortical thickness

Colourimetric maps were superimposed to show differences in cortical thickness between groups and hemispheres (Fig. 1A). Overall, cortical thickness was greater in SDS patients, both in the left (+10%) and in the right (+15%) hemisphere and significantly increased in the temporal (left and right, $p = 0.04$) and right parietal ($p = 0.03$) lobes. The greatest increases were observed in the left limbic-anterior cingulate cortex (≥43%, $p < 0.0004$). Cortical thickness resulted to be increased in all the BA of the right frontal, significantly increased in BA44. Only in the left hemisphere of Broca's area (BA44, BA45) did SDS patients show a thinner cortical thickness than controls (Fig. 1B).

3.3. fMRI: blood oxygen level dependent signals

3.3.1. Brain activation during the Stroop task

During fMRI the activated brain areas in SDS subjects differed from, and were smaller than those activated in controls, both when performing a task (Fig. 2I) and in the resting state (Fig. 2II). SDS subjects performed the Stroop task at the same time as controls, but with more errors (for both congruent and incongruent stimuli) (Table 2A).

3.3.2. Brain activation at-rest: the default mode network

ICA of the BOLD signal in the resting condition showed different, and reduced, neuronal network recruitment in SDS (Table 2B).

3.4. White matter connectivity

DTI showed large, consistent and significant differences between SDS and control subjects, in both FA and MD (in SDS, +37% and +35% respectively, $p < 0.001$) (Fig. 3A; SI Table 1)

FA data were subjected to voxelwise TBSS analysis. The analysis identified six clusters where FA was significantly higher in SDS subjects than in controls.

For the six clusters identified, the higher FA values in the SDS group resulted from increased diffusion not only along the primary direction, but also along the secondary and tertiary directions.

The connectivity maps representing the most likely pathways extending to and from each cluster identified in the TBSS analysis are shown in Fig. 3B.

3.5. Brain anomalies and cognitive performance

SDS subjects showed several cortical areas whose thickness shows a significant negative correlation with cognitive performance. This was particularly evident in the temporal, parietal and cingulate regions, whose thickness correlated negatively with performance in verbal reasoning, perceptual reasoning and memory. With regard to the six clusters where white matter was significantly altered, FA values in cluster 1 (fronto-callosal) correlated with a worse performance in executive functions; cluster 2 (frontal/external capsulae) and cluster 5 (anterior/medial/temporal) correlated negatively with verbal performance; cluster 3 (fronto-parietal) negatively correlated with perceptual skills, verbal/non-verbal memory and executive function; FA values in cluster 4 (pontine) correlated negatively with visual–motor integration function and cluster 6 with perceptual skills (Table 3; SI Table 2).

4. Discussion

The results of this study show diffuse alterations in grey and white matter associated with cognitive impairment in SDS subjects. To our knowledge, this is the first study that concurrently investigates brain structure and cognitive performance in SDS patients and healthy subjects, matched for age and gender.

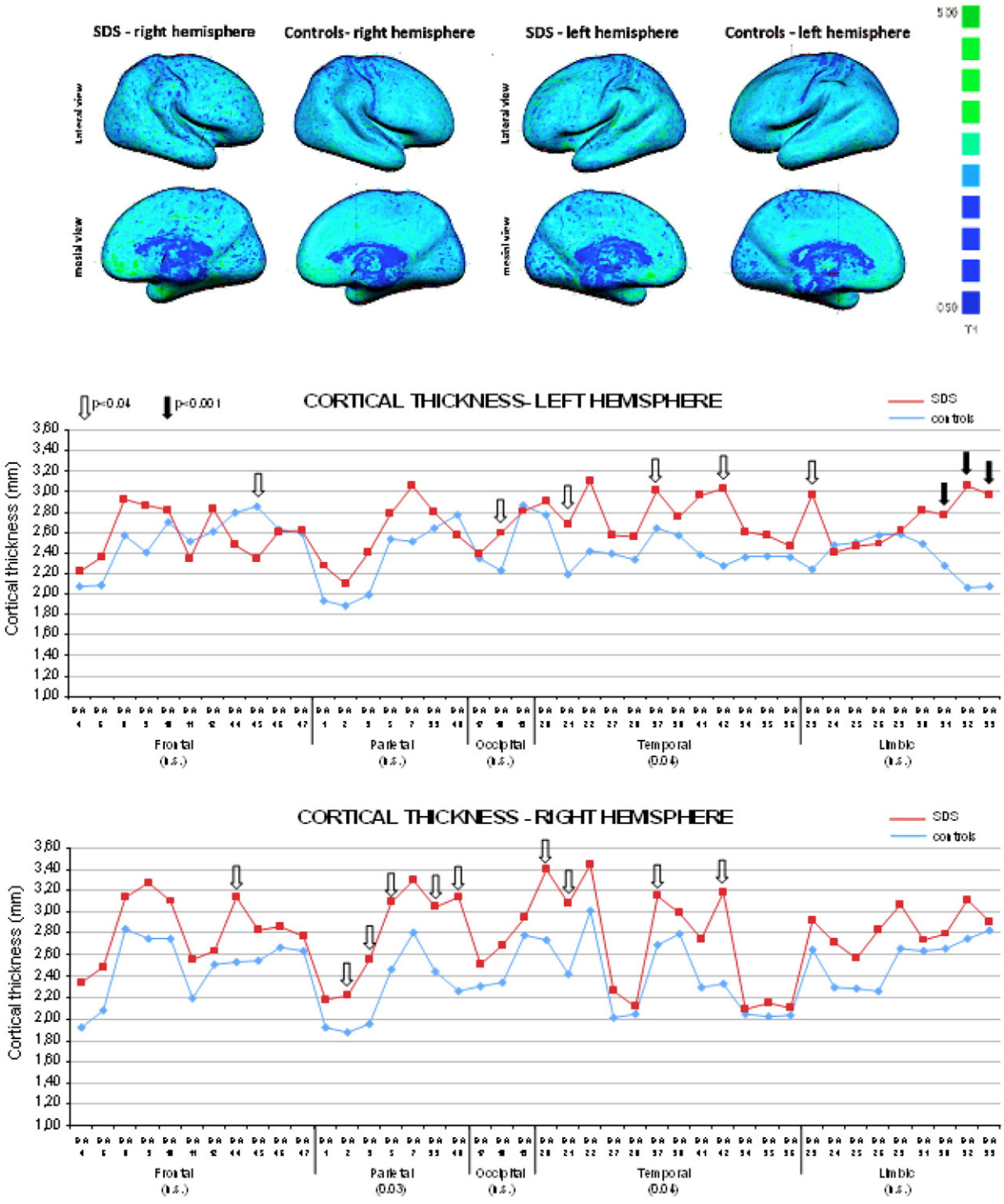

Fig. 1. Differences in cortical thickness between groups and hemispheres. A) Right and left hemispheres, 3D reconstruction in SDS and control subjects. Upper row: lateral views. Lower row: mesial views. Colourimetric maps show differences in cortical thickness between groups and hemispheres (dark blue: 0.5 mm; green: 5 mm). B) The graphs show the mean values of the cortical thickness registered in all the Brodmann areas (BAs) in SDS and in controls. The following BA resulted to be significantly increased in SDS: in the frontal lobe—right BA44 +12% ($p = 0.04$); in the parietal lobe—right BA2 +18% ($p = 0.03$), BA3 +30% ($p = 0.005$), BA5 +26% ($p = 0.02$), BA39 +20% ($p = 0.03$), BA40 +39% ($p = 0.03$); in the temporal lobe—right BA20 +24% ($p = 0.007$), BA21 +27% ($p = 0.007$), BA37 +17% ($p = 0.02$), BA42 +36% ($p = 0.02$); in the temporal lobe—left BA21 +22% ($p = 0.01$), BA22 +29% ($p = 0.02$), BA37 +14% ($p = 0.01$), BA42 +33% ($p = 0.02$); in the occipital lobe—left BA18 +16% ($p = 0.04$); and in the limbic—left BA23 +33% ($p = 0.0001$), BA31 +22% ($p = 0.003$), BA32 +49% (0.0001), BA33 +43% (0.0004). Only in the frontal lobe—left BA45 showed a thinner cortical thickness in SDS subjects (−18%, $p = 0.01$), than that in controls.

Cognitive function in SDS subjects was confirmed to be impaired, scoring in the lower normal range as regards both verbal and perceptual reasoning. Only some basic functions were found to be relatively well preserved (e.g. geometric forms to be pencil-copied in the visual–motor integration test, picture completion, puzzle construction in the object assembly subtest), while higher level functions dependent on planning and sequential responses were significantly impaired, both in the verbal and non-verbal tasks (like the picture arrangement subtest, which requires the integration of visual perceptual ability, social understanding and higher order thinking and planning). Attention and

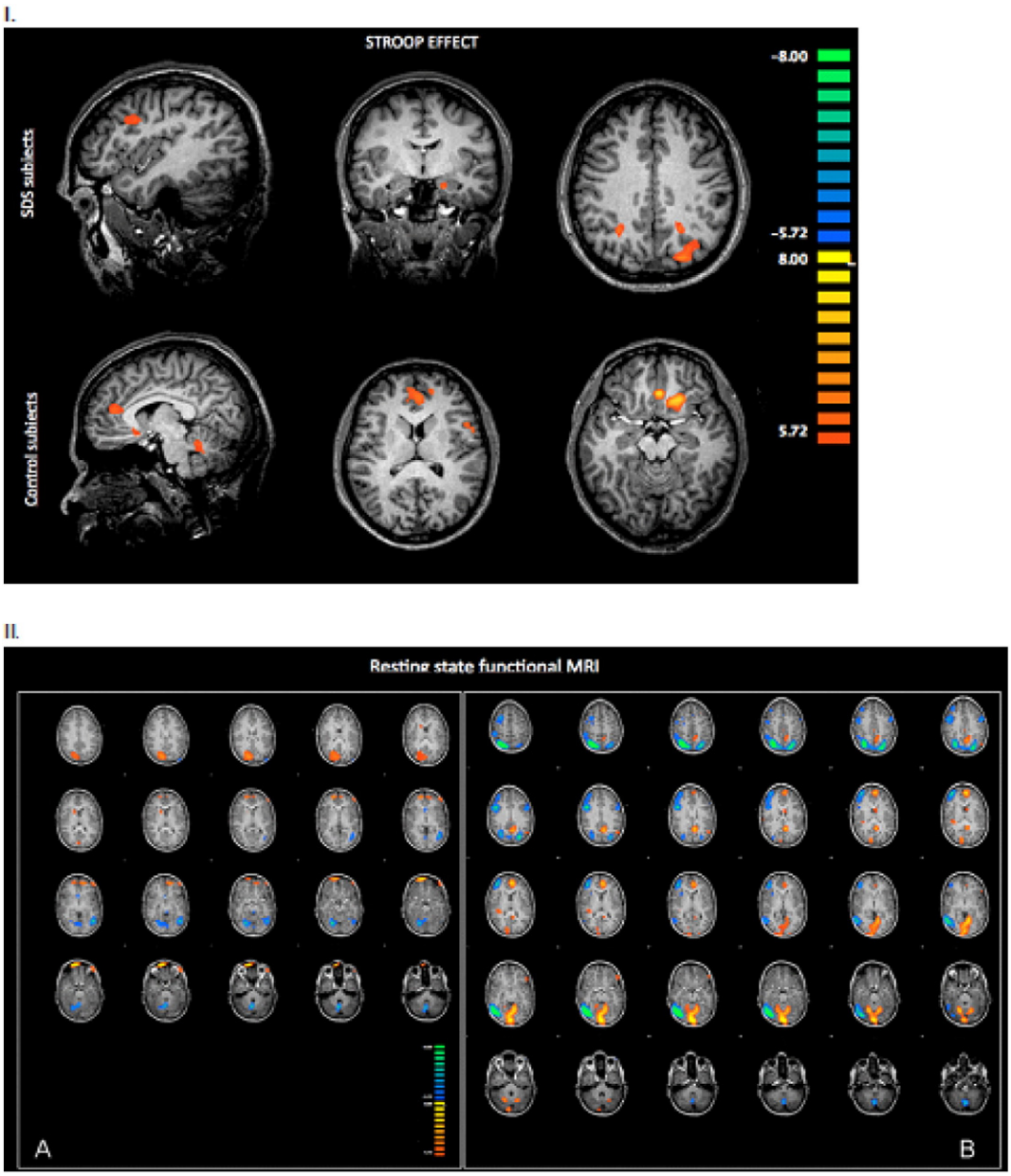

Fig. 2. SDS vs. control subject pattern of activation in the Stroop effect and in resting state. fMRI maps superimposed on 3D T1 weighted anatomical images ($p < 0.05$) (radiological view: R = L). I. The upper row represents findings of random effect group analysis (SDS vs. controls) in SDS subjects, i.e. brain activation in the middle left frontal gyrus, left precuneus and left hippocampus. In the lower panel random effect group analysis (controls vs. SDS) in control subjects shows brain activation in the anterior cingulate cortex, in the orbital cortex and in the left inferior frontal gyrus. II. The panel represents findings of independent component analysis (ICA) of BOLD fMRI signal in resting state activity (panel A: SDS; panel B: controls). ICA maps are superimposed on a T1 weighted anatomical template. SDS subjects show different and reduced functional connectivity networks within the default mode network (DMN) in resting state activity ($p < 0.001$).

memory were also found to be impaired. As reported by parents, school performance and socialization were low in relation to age, while emotional or behavioural problems were not present.

4.1. Abnormal cortical thickness

Cortical thickness is considered to be a good indicator of grey matter maturation, sensitive to developmental change in typically developing and clinical populations. Cortical thickness correlates with intelligence, shifting from a negative correlation in early childhood to a positive correlation in late childhood and beyond (Shaw et al., 2006; Shaw et al., 2008; Luders et al., 2009). Grey matter maturation is accomplished after a thinning of the cortical mantle and is probably due to synaptic pruning (Shaw et al., 2008; Tamnes et al., 2010), adolescence being the time when the greatest cortical thinning occurs (Shaw et al., 2006; Tamnes et al., 2010). Previous studies have shown a correlation between cortical thickness and development disorders such as attention deficit hyperactivity disorder (Batty et al., 2010), autism (Wallace et al., 2010) and heavy prenatal alcohol exposure (Sowell et al., 2008).

With the combined use of MRI, functional MRI and DTI, we explored several aspects of brain structure. In SDS patients we found that cortical thickness was generally increased in all areas on both sides, significantly so in several areas of the right parietal, right and left temporal, left limbic, left occipital and right frontal lobes. The only exception to this trend was found in Broca's area of the left frontal lobe, where it was significantly reduced (−18%). The

Table 2
Functional brain activity differences in SDS and controls. The region of activation is shown as well as the side, the peak location in Talairach coordinates (x,y,z) and the number of activated voxels. The activation clusters were identified after carrying out a t-test ($p < 0.05$) and a Z-test ($p < 0.001$, $Z = 3.3$).

A. Functional MRI BOLD signal and performance (errors, reaction time) during the Stroop test

SDS	BA	Side	Peak (x,y,z)	t	k	Total errors median (range)	Incongruent tasks median (range)	Reaction time (msec.) mean (sd)
Inferior parietal gyrus	7	R	31,−51,29	6.37	602			
Medial frontal gyrus	9	L	−20,33,23	6.43	1741			
Precuneus	31	L	−17,−45,41	6.51	3121			
Hippocampus	38	L	−19,−8,−12	6.31	452			
						9 (3–13)[a]	6 (2–11)[a]	706.65 (331.56)
Controls								
Anterior cingulate	32	R	7,51,14	9.47	2991			
Superior frontal gyrus	8	R	1,27,−10	8.34	368			
Orbital gyrus	11	L	−11,21,−10	8.51	1247			
Superior parietal gyrus	5	L	−29,−63,53	7.21	582			
Inferior frontal gyrus (Broca)	44	L	−50,39,2	9.38	1933			
						5 (2–7)	2 (1–6)	766.63 (392.9)

B. Functional MRI BOLD signal during "resting state" condition and ICA analysis

SDS		Side	Peak (x,y,z)	z.ica	k
Lingual gyrus	18	R	21,−68,−12	−3.2	678
Superior frontal gyrus	8	R	15,55,3	2.7	358
Cerebellum	–	L	−3,−74,−42	−3.1	1575
Inferior occipital gyrus	19	L	−42,−59,−3	−2.71	601
Controls					
Inferior occipital gyrus	19	R	33,−74,−12	−4.01	6306
Inferior frontal gyrus	45	R	36,7,27	−2.84	710
Medial frontal gyrus	9	R	39,46,12	−2.6	1178
Superior parietal gyrus	5	R	21,−68,51	−5.8	6596
Cerebellum	–	R	12,-59-21	3.2	613
Cerebellum	–	L	−3,−86,−15	4.26	4748
Superior frontal gyrus	8	L	−3,49,9	2.75	773
Retrosplenial cingulate cortex	23	L	−6,−50,18	2.42	404
Inferior parietal gyrus	7	L	−24,−77,33	−3	2855

BA = Brodmann area; BOLD = blood oxygen level dependent; R = right; L = left; k = number of activated voxels; ICA = independent component analysis.
[a] Comparison SDS vs. controls: $p = 0.002$

areas with the greatest differences were in the cingulate cortex, in the parietal and temporal lobes. The thickening correlated negatively with cognitive performance scores.

Cognitive development, as well as cortical development, in children with SDS seems to lag behind that of normal children, but we cannot say whether this difference is related to delay in cortical maturation (alterations of neuronal pruning) or is the endpoint of the disease.

4.2. Lack of activation in cingulate cortex during an attentional task and at rest

The BOLD signal also showed differences between the two groups of subjects: the brain areas activated during the Stroop task, and remaining active in the resting state, were different, fewer in number and smaller in SDS subjects. While control subjects showed extensive activation of the prefrontal areas known to be important in executive control and selective attention (prefrontal areas) (Vloosvijk et al., 2010), in SDS children the dorsolateral prefrontal cortex and the anterior cingulate cortex were not activated at all and activation of the prefrontal areas was rather low. This correlates with the Stroop test results, where SDS subjects made more errors, although their speed of execution was comparable to that of normal subjects.

In rs-MRI, the posterior cingulate cortex was activated in controls but not in SDS patients. The posterior cingulate cortex shows increased activity when individuals retrieve autobiographical memories or plan for the future, as well as during unconstrained 'rest' when activity in the brain is 'free-wheeling', and seems to be a key node in the default mode network. Our results are similar to those shown in a range of neurological disorders, both in adults and in children, including Alzheimer's disease, schizophrenia, autism, depression and attention deficit hyperactivity disorder (Leech and Sharp, 2013).

4.3. Diffusion abnormalities in white matter fibres

As regards white matter integrity, age-related changes in its microstructure have been well documented: they most consistently show linear increases in FA and decreases in MD with age during adolescence (Catani et al., 2006; Bava et al., 2010). This trend correlates with cognitive level.

In several diseases during adolescence, FA was found to progressively decrease: in Sturge–Weber syndrome (Alkonyi et al., 2011), in myotonic dystrophy type 1 (Wozniak et al., 2011) and in autism (Shukla et al., 2011), as well as in children suffering from early deprivation (Govindan et al., 2010a). In Tourette syndrome, FA has been seen to increase with tics (Govindan et al., 2010b).

We measured FA, MD, RD and PD. All these parameters, and particularly FA and MD, were significantly and homogeneously increased (+30%) in SDS subjects. The biophysical meaning of diffusion abnormalities in white matter is not yet fully understood. Values of FA can be affected by many variations in the white matter structure, including changes in intra- and extra-cellular volume, permeability of cell membranes, fibre coherence, and axonal loss (Pierpaoli and Basser, 1996). DTI studies commonly attribute an increase in FA to an increase in density, more coherent organization, and greater myelination of fibres (Mori and Zhang, 2006). The increase in FA observed in our SDS group was also associated with an increase in diffusion along the secondary and tertiary directions (data not shown). This rise in diffusion along the secondary and tertiary directions may represent an abnormally higher degree of neuronal branching within the white matter pathways

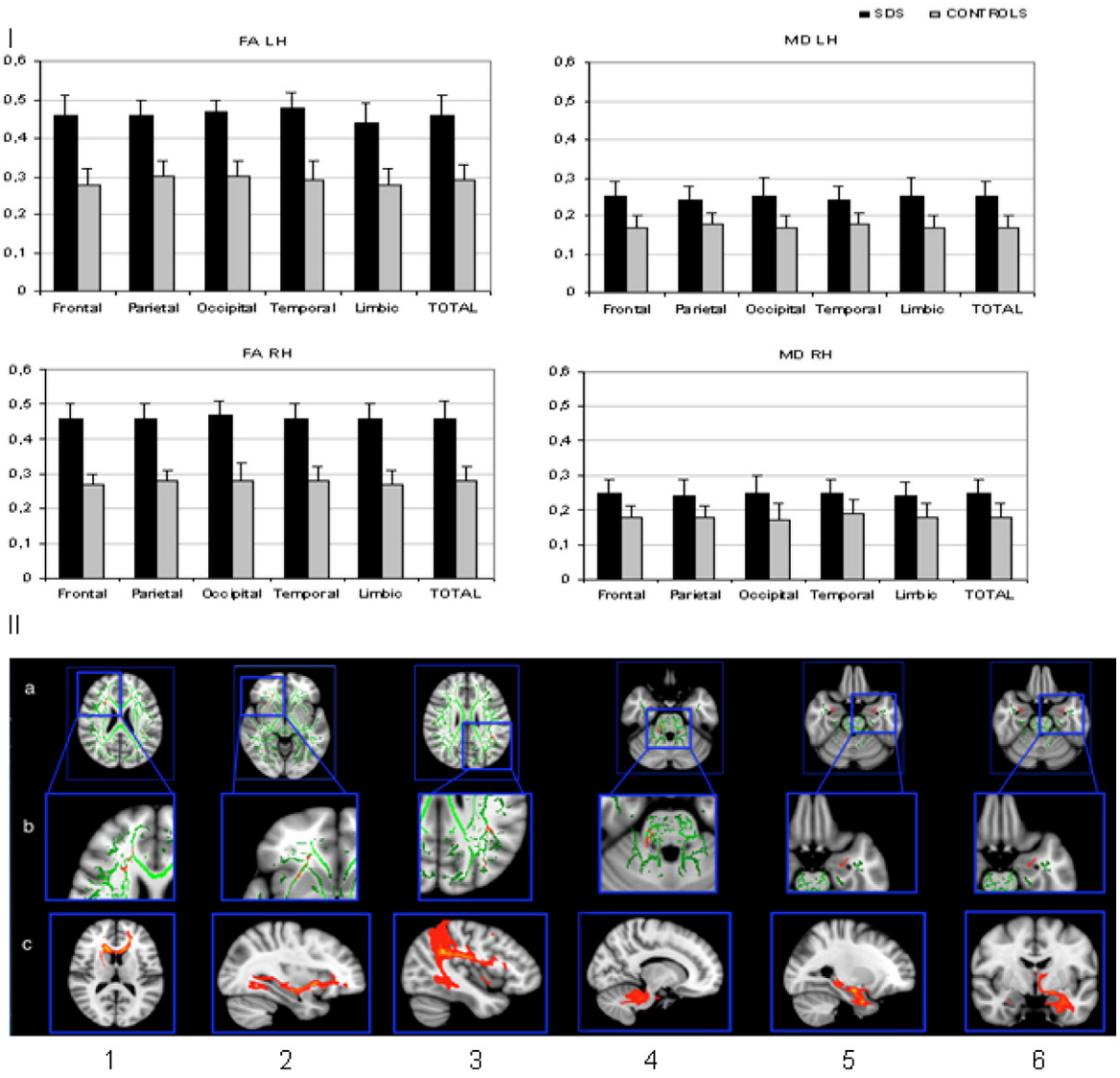

Fig. 3. Diffusion tensor imaging (DTI) and Tract-based Spatial Statistics (TBSS) analyses. A. DTI analysis: differences in fractional anisotropy (FA) and mean diffusivity (MD) between SDS and control groups (LH = left hemisphere; RH = right hemisphere). B. a) TBSS analysis showing the mean FA skeleton (green) and regions with statistically significant differences between SDS and control groups (red), displayed on the MNI152 brain (radiological view: R = L). b) Detailed view. c) Slices showing the connectivity distribution of fibres originating from each of the areas of FA difference shown immediately above. Connectivity maps representing the paths extending to and from each cluster identified in the TBSS analysis. Fibre paths are displayed on the representative target FA image to which all other images are registered. 1) The cluster in the fronto-callosal region [anterior cingulated, peak (x,y,z) 17,31,16; k 785, $p < 0.02$] formed part of the bilateral white matter connections in the pre-frontal regions, through the genu of the corpus callosum and the anterior cingulum. 2) The cluster in the right frontal–external capsulae [fronto-occipital fasciculus, peak (x,y,z) 23,35,−1; k 4435, $p < 0.02$] formed part of the pathways interconnecting the ipsilateral frontal and occipital regions through the fronto-occipital fasciculus. 3) The cluster in the left fronto-parietal region [arcuate fasciculus, peak (x,y,z) −42,−44,32; k 375, $p < 0.03$] formed part of the pathways interconnecting the frontal and temporal lobes, which give rise to the arcuate fasciculus. 4) The cluster in the right pontine region [ponto-cerebellar fasciculus, peak (x,y,z) 18,−32,−32; k 785, $p < 0.03$] formed part of the pathway interconnecting the right cerebellar hemisphere through the ponto-cerebellar fasciculus. 5) The clusters in the anterior medial temporal lobes [inferior longitudinal fasciculus, peak (x,y,z) −29,−3,−24; k 139, $p < 0.03$] formed part of the pathways interconnecting the hippocampus, the amygdala and the inferior longitudinal fasciculus. 6) The cluster in the left anterior medial temporal lobe [limbic, peak (x,y,z) −27,−4,−23; k 139, $p < 0.02$] formed part of the pathway interconnecting the hippocampus and amygdala to the ipsilateral thalamus.

underlying the fronto-temporal and occipito-parietal regions. It may also be representative of the clusters' location, i.e. a region with a high density of crossing fibres.

4.4. Neural connections between prefrontal and parieto-occipital areas with the striatum and the cerebellum

We then used TBSS to assess connectivity. This method has been shown to be sensitive to changes in white matter diffusion, even in relatively small samples (fewer than 30 subjects) like ours (Focke, 2008). In SDS patients, we identified six clusters of altered fibres interfering with inter- and intra-hemispheric connections. All the regions involved in these clusters are associated with neural connections that link the prefrontal and parieto-occipital areas with the striatum and the cerebellum. The mean fractional anisotropy values of these tracts show a significant negative correlation with the cognitive performance of SDS patients. FA values in the right frontal–external capsulae (inferior fronto-occipital fasciculus—cluster 2) and in the anterior–medial–temporal lobe (inferior longitudinal fasciculus—cluster 5) are negatively correlated with verbal performance; these bundles functionally connect the occipital and the orbito-frontal cortex, through the uncinate fasciculus and the occipital cortex, with the amygdala and temporal lobe respectively. These circuits play an important role in the feed forward sequence transmitted from the visual to the fronto-temporal areas (language) and limbic system (memory and emotion) (Han et al., 2013).

Table 3
Main effects of increased cortical thickness and altered connectivity on cognitive performance in Shwachman-Diamond patients. Correlation analysis was performed between cognitive test scores, cortical thickness and altered clusters of white matter. Only correlations greater than 0.70 were reported.The results indicate the lobe, Brodmann area (BA) and hemisphere (R = right; L = left) where a negative correlation was found.

	Frontal	Parietal	Temporal	Limbic	Cluster n.1 Fronto-callosal (anterior cingulate) BA24-32	Cluster n.2 Frontal/Ext. capsulae (fronto-occipital fasciculus) BA11-20-18	Cluster n.3 Fronto-parietal (arcuate fasciculus) BA7-37-39	Cluster n.4 Pontine (ponto-cerebellar fasciculus) BA4-6	Cluster n.5 Anterior medial temporal (inferior longitudinal fasciculus) BA20-21-38	Cluster n.6 Anterior medial temporal (limbic) BA45-38
Cognitive skills										
Verbal	BA44−RH−0.76 (0.03)		BA20−RH−0.74 (0.03)			−0.71 (0.04)			−0.71 (0.04)	
Perceptual		BA5- RH-0.77(0.02)	BA37−RH -0.87(0.01)	BA32-LH−0.76 (0.03)			−0.81 (0.02)			−0.69 (0.04)
		BA39-LH-0.71(0.04)	BA20−RH -0.86(0.01)							
			BA21−RH -0.86(0.01)							
			BA42−RH -0.70(0.04)							
Visual–motor integration								−0.87 (0.03)		
Memory skills										
Composite memory (Verbal/non verbal)				BA23-LH−0.79 (0.03)			−0.74 (0.03)			
Working memory			BA42-LH−0.89 (0.01)							
Executive functions % perseverative errors					0.72 (0.04)		0.80 (0.03)			

4.5. Impact of altered thickness and connectivity on cognition

The tract in the fronto-parietal region identified as cluster 3 negatively correlated with verbal and non-verbal memory, perceptual skills and executive functions. Several clinical manifestations have been related to alterations in cortical areas and white matter tracts of the parietal lobes. Reduced FA in anterior segment of arcuate fasciculus correlates with the severity of reading difficulties in children with dyslexia and reduced FA in the parietal connections was associated with developmental dyscalculia in normal developing children (Catani et al., 2012). SDS subjects seem to suffer from a diffuse (rather than a focal) anomaly, in areas that are important for global intellectual functioning. What we found in SDS subjects is consistent with the Parieto-Frontal Integration model (Jung and Haier, 2007). Altered thickness and connectivity impairment occurred in areas that are essential for the processing of visual and auditory inputs: the extrastriatal cortex (Ba18), the fusiform gyrus (BA37) and the middle temporal gyrus (BA21). We also found white matter anomalies in the angular gyrus of the parietal cortex (BA39) and in the upper parietal gyrus (BA7), where symbolic interpretation and abstract thinking take place. The ability to recognize future consequences resulting from current actions, and to choose between actions, resides in the frontal lobes. Here we found two areas crossed by abnormal white matter fascicles, which showed thickening in one case (anterior cingulate, BA32) and thinning in the other (Broca's area, BA45). This thinning seems to be particularly important, for two reasons: it is the only area of thinning, all the other areas being thickened, and it is the area within the frontal lobe which is still in the maturation stage in healthy adolescents, while the other brain areas are already becoming thinner. These results point to a developmental anomaly in SDS children and add new information on brain abnormalities. None of the previous studies chose cortical thickness to explore grey matter status, and DTI and TBSS to investigate white matter integrity. Two previous MRI studies used volumetric measures and reported reduced brain volume in SDS (Toiviainen-Salo et al., 2008; Booij et al., 2013). These and our results, although difficult to compare, are not in disagreement. Even if grey matter volume (GMV) is a composite of two traits – surface area (SA) and cortical thickness (CT) – it has been shown that CT and SA are independent, heritable but not genetically correlated and arise from different progenitor cells which create glial cells and neurons at distinct points in corticogenesis (Jalbrzikowsky et al., 2013). GMV is influenced more by SA than by CT, which provides a possible explanation for the findings of increased CT and decreased volume in the same brain region, as showed by imaging genetics studies and in neurodevelopmental disorders, such as dyslexia (Panizzon et al., 2009; Winkler et al., 2010; Ma et al., 2015).

4.6. Limitations

The lack of longitudinal data represents a significant limitation of this study. Undoubtedly more detailed knowledge regarding the evolution of these dysfunctions would make it possible to address them better, with specific intervention programmes aimed at reducing the impairment.

Moreover, our group of patients is relatively small, though it accounts for 50% of this age group in the Italian SDS Registry. In the presence of so rare disease, a larger study could be feasible only as a multicentre international trial.

It would be relevant to know the relationship between the genetic defect and the identified brain anomalies. This might provide a means to elucidate some of the biological mechanisms underlying this syndrome.

5. Conclusions

Our study thus provides new information about cognitive and cerebral dysfunctions in SDS. We assessed pre-adolescent patients and we cannot say whether brain maturation lags behind, or whether the defects that we found are stable.

We still do not know what links the SBDS gene with the cerebral abnormalities that we found. We may only speculate that a link exists, and confirm that cerebral abnormalities originate from the altered gene function.

Conflict of interest

The study was supported (grant n. 0409) in part by the Italian Shwachman Syndrome Association (AISS). The sponsor had no role in the study design, data collection, data analysis, data interpretation, or writing of the report. The corresponding author had full access to all the data in the study, and all co-authors had final responsibility for the decision to submit for publication.

Acknowledgements

The study was supported by a grant (n. 0409) from the Italian Shwachman Syndrome Association (AISS). We thank Patrizia Esmanech for doing the testing examination of some of the participants with great dedication; Ilaria Meneghelli and Marianna Passiu for their administrative assistance in the Ethical Committee approval; Raffaella Rumiati for her encouragement during the study; Daniel Sher for helping in the production of the first English draft; and Peter Mead for the final revision of the English text.

Appendix A. Supplementary data

Supplementary data to this article can be found online at http://dx.doi.org/10.1016/j.nicl.2015.02.014.

References

Achenbach, T., 1991. Child Behavior Checklist. University of Vermont, Dept. of Psychiatry, Burlington, VT.
Alkonyi, B., et al., 2011. Focal white matter abnormalities related to neurocognitive dysfunction: an objective diffusion tensor imaging study of children with Sturge–Weber syndrome. Pediatr. Res. 69 (1), 74–79. http://dx.doi.org/10.1203/PDR.0b013e3181fcb28520856167.
Bartolomeo, P., 2011. The quest for the 'critical lesion site' in cognitive deficits: problems and perspectives. Cortex 47 (8), 1010–1012. http://dx.doi.org/10.1016/j.cortex.2010.11.00721185556.
Batty, M.J., et al., 2010. Cortical gray matter in attention-deficit/hyperactivity disorder: a structural magnetic resonance imaging study. J. Am. Acad. Child Adolesc. Psychiatry 49 (3), 229–238. http://dx.doi.org/10.1016/j.jaac.2009.11.00820410712.
Bava, S., et al., 2010. Longitudinal characterization of white matter maturation during adolescence. Brain Res. 1327, 38–46. http://dx.doi.org/10.1016/j.brainres.2010.02.06620206151.
Beery, K.E., Buktenica, N.A., 1997. The Beery–Buktenica Developmental Test of Visual–Motor Integration fourth edition. NCS Pearson, Minneapolis.
Bodian, M., Sheldon, W., Lightwood, R., 1964. Congenital hypoplasia of the exocrine pancreas. Acta Paediatr 53, 282–293. http://dx.doi.org/10.1111/j.1651-2227.1964.tb07237.x14158482.
Boocock, G.R., et al., 2003. Mutations in SBDS are associated with Shwachman–Diamond syndrome. Nat. Genet. 33 (1), 97–101. http://dx.doi.org/10.1038/ng106212496757.
Booij, J., Reneman, L., Alders, M., Kuijpers, T.W., 2013. Increase in central striatal dopamine transporters in patients with Shwachman–Diamond syndrome: additional evidence of a brain phenotype. Am. J. Med. Genet. A 161A (1), 102–107. http://dx.doi.org/10.1002/ajmg.a.3568723239620.
Brodmann, K., 1909. Vergleichende Lokalisationslehere der Grosshimrinde in ihren Prinzipien dargestellt auf Grund des Zellenbaues. J.A. Barth, Leipzig.
Catani, M., ffytche, D.H., 2005. The rises and falls of disconnection syndromes. Brain 128 (10), 2224–2239. http://dx.doi.org/10.1093/brain/awh62216141282.
Catani, M., 2006. Diffusion tensor magnetic resonance imaging tractography in cognitive disorders. Curr. Opin. Neurol. 19 (6), 599–606. http://dx.doi.org/10.1097/01.wco.0000247610.44106.3f17102700.
Catani, M., Mesulam, M., 2008. What is a disconnection syndrome? Cortex 44 (8), 911–913. http://dx.doi.org/10.1016/j.cortex.2008.05.00118603236.
Catani, M., et al., 2012. Beyond cortical localization in clinico-anatomical correlation. Cortex 48 (10), 1262–1287. http://dx.doi.org/10.1016/j.cortex.2012.07.00122995574.
Chanraud, S., Zahr, N., Sullivan, E.V., Pfefferbaum, A., 2010. MR diffusion tensor imaging: a window into white matter integrity of the working brain. Neuropsychol. Rev. 20 (2), 209–225. http://dx.doi.org/10.1007/s11065-010-9129-720422451.
Cipolli, M., 2001. Shwachman–Diamond syndrome: clinical phenotypes. Pancreatology 1 (5), 543–548. http://dx.doi.org/10.1159/00005585812120235.

Focke, N.K., et al., 2008. Voxel-based diffusion tensor imaging in patients with mesial temporal lobe epilepsy and hippocampal sclerosis. Neuroimage 40 (2), 728–737. http://dx.doi.org/10.1016/j.neuroimage.2007.12.03118261930.
Freilich, E.R., Gaillard, W.D., 2010. Utility of functional MRI in pediatric neurology. Curr. Neurol. Neurosci. Rep. 10 (1), 40–46. http://dx.doi.org/10.1007/s11910-009-0077-720425225.
Friston, K.J., et al., 1994. Statistical parametric maps in functional imaging: a general linear approach. Hum. Brain Mapp. 2 (4), 189–210. http://dx.doi.org/10.1002/hbm.460020402.
Goh, S., et al., 2011. Neuroanatomical correlates of intellectual ability across the life span. Dev. Cogn. Neurosci. 1 (3), 305–312. http://dx.doi.org/10.1016/j.dcn.2011.03.00122436512.
Govindan, R.M., Makki, M.I., Wilson, B.J., Behen, M.E., Chugani, H.T., 2010a. Abnormal water diffusivity in corticostriatal projections in children with Tourette syndrome. Hum. Brain Mapp. 31 (11), 1665–1674. http://dx.doi.org/10.1002/hbm.2097020162597.
Govindan, R.M., Behen, M.E., Helder, E., Makki, M.I., Chugani, H.T., 2010b. Altered water diffusivity in cortical association tracts in children with early deprivation identified with Tract-Based Spatial Statistics (TBSS). Cereb. Cortex 20 (3), 561–569. http://dx.doi.org/10.1093/cercor/bhp122.
Han, Z., et al., 2013. White matter structural connectivity underlying semantic processing: evidence from brain damaged patients. Brain 136 (10), 2952–2965. http://dx.doi.org/10.1093/brain/awt20523975453.
Heaton, R.K., et al., 1981. Wisconsin Card Sorting Test. Assessment Resources, Odessa, Florida.
Hegarty, C.E., et al., 2012. Anterior cingulate activation relates to local cortical thickness. Neuroreport 23 (7), 420–424. http://dx.doi.org/10.1097/WNR.0b013e3283525a9522440976.
Hyvärinen, A., Oja, E., 2000. Independent component analysis: algorithms and applications. Neural Netw. 13 (4–5), 411–430. http://dx.doi.org/10.1016/S0893-6080(00)00026-510946390.
Jalbrzikowski, M., et al., 2013. Structural abnormalities in cortical volume, thickness, and surface area in 22q11.2 microdeletion syndrome: relationship with psychotic symptoms. Neuroimage Clin. 3, 405–415. http://dx.doi.org/10.1016/j.nicl.2013.09.01324273724.
Jones, S.E., Buchbinder, B.R., Aharon, I., 2000. Three-dimensional mapping of cortical thickness using Laplace's equation. Hum. Brain Mapp. 11 (1), 12–32. http://dx.doi.org/10.1002/1097-0193(200009)11:1<12::AID-HBM20>3.0.CO;2-K10997850.
Jung, R.E., Haier, R.J., 2007. The parieto-frontal integration theory (P-FIT) of intelligence: converging neuroimaging evidence. Behav. Brain Sci. 30 (2), 135–154. http://dx.doi.org/10.1017/S0140525X0700118517655784.
Kamoda, T., et al., 2005. A case of Shwachman–Diamond syndrome presenting with diabetes from early infancy. Diabetes Care 28 (6), 1508–1509. http://dx.doi.org/10.2337/diacare.28.6.150815920082.
Kent, A., Murphy, G.H., Milla, P., 1990. Psychological characteristics of children with Shwachman syndrome. Arch. Dis. Child. 65 (12), 1349–1352. http://dx.doi.org/10.1136/adc.65.12.13491702966.
Kerr, E.N., Ellis, L., Dupuis, A., Rommens, J.M., Durie, P.R., 2010. The behavioral phenotype of school-age children with Shwachman Diamond syndrome indicates neurocognitive dysfunction with loss of Shwachman–Bodian–Diamond syndrome gene function. J. Pediatr. 156 (3), 433–438. http://dx.doi.org/10.1016/j.jpeds.2009.09.02619906387.
Leech, R., Sharp, D.J., 2013. The role of posterior cingulated cortex in cognition and disease. Brain 137 (1), 12–32.
Lu, L.H., Dapretto, M., O'Hare, E.D., et al., 2009. Relationships between brain activation and brain structure in normally developing children. Cereb. Cortex 19 (11), 2595–2604. http://dx.doi.org/10.1093/cercor/bhp01119240138.
Luders, E., Narr, K.L., Thompson, P.M., Toga, A.W., 2009. Neuroanatomical correlates of intelligence. Intelligence 37 (2), 156–163. http://dx.doi.org/10.1016/j.intell.2008.07.00220160919.
Ma, Y., et al., 2015. Cortical thickness abnormalities associated with dyslexia, independent of remediation status. Neuroimage Clin. 7, 177–186. http://dx.doi.org/10.1016/j.nicl.2014.11.00525610779.
MacLeod, C.M., 1991. Half a century of research on the Stroop effect: an integrative review. Psychol. Bull. 109 (2), 163–203. http://dx.doi.org/10.1037/0033-2909.109.2.1632034749.
Mori, S., Zhang, J., 2006. Principles of diffusion tensor imaging and its applications to basic neuroscience research. Neuron 51 (5), 527–539. http://dx.doi.org/10.1016/j.neuron.2006.08.01216950152.
Panizzon, M.S., et al., 2009. Distinct genetic influences on cortical surface area and cortical thickness. Cereb. Cortex 19 (11), 2728–2735. http://dx.doi.org/10.1093/cercor/bhp02619299253.
Perobelli, S., Nicolis, E., Assael, B.M., Cipolli, M., 2012. Further characterization of Shwachman–Diamond syndrome: psychological functioning and quality of life in adult and young patients. Am. J. Med. Genet. 158A (3), 567–573. http://dx.doi.org/10.1002/ajmg.a.35211.
Pierpaoli, C., Basser, P.J., 1996. Toward a quantitative assessment of diffusion anisotropy. Magn. Reson. Med. 36 (6), 893–906. http://dx.doi.org/10.1002/mrm.19103606128946355.
Reynolds, C.R., Bigler, E.D.., 1994. Test of Memory and Learning (TOMAL). PRO-ED, Austin, Texas.
Ross, E.D., 2010. Cerebral localization of functions and the neurology of language: fact versus fiction or is it something else? Neuroscientist 16 (3), 222–243. http://dx.doi.org/10.1177/10738584093498992013933 4.
Schmithorst, V.J., Yuan, W., 2010. White matter development during adolescence as shown by diffusion MRI. Brain Cogn. 72 (1), 16–25. http://dx.doi.org/10.1016/j.bandc.2009.06.00519628324.
Shaw, P., et al., 2006. Intellectual ability and cortical development in children and adolescents. Nature 440 (7084), 676–679. http://dx.doi.org/10.1038/nature0451316572172.
Shaw, P., et al., 2008. Neurodevelopmental trajectories of the human cerebral cortex. J. Neurosci. 28 (14), 3586–3594. http://dx.doi.org/10.1523/JNEUROSCI.5309-07.200818385317.
Shukla, D.K., Keehn, B., Smylie, D.M., Müller, R.A., 2011. Microstructural abnormalities of short-distance white matter tracts in autism spectrum disorder. Neuropsychologia 49 (5), 1378–1382. http://dx.doi.org/10.1016/j.neuropsychologia.2011.02.02221333661.
Shwachman, H., Diamond, L.K., Oski, F.A., Khaw, K.T., 1964. The syndrome of pancreatic insufficiency and bone marrow dysfunction. J. Pediatr. 65, 645–663. http://dx.doi.org/10.1016/S0022-3476(64)80150-514221166.
Smith, S.M., et al., 2006. Tract-based spatial statistics: voxelwise analysis of multi-subject diffusion data. Neuroimage 31 (4), 1487–1505. http://dx.doi.org/10.1016/j.neuroimage.2006.02.02416624579.
Sowell, E.R., et al., 2008. Abnormal cortical thickness and brain–behavior correlation patterns in individuals with heavy prenatal alcohol exposure. Cereb. Cortex 18 (1), 136–144. http://dx.doi.org/10.1093/cercor/bhm03917443018.
Tamnes, C.K., et al., 2010. Brain maturation in adolescence and young adulthood: regional age-related changes in cortical thickness and white matter volume and microstructure. Cereb. Cortex 20 (3), 534–548. http://dx.doi.org/10.1093/cercor/bhp11819520764.
Todorovic-Guid, M., et al., 2006. A case of Shwachman–Diamond syndrome in a male neonate. Acta Paediatr. 95 (7), 892–893. http://dx.doi.org/10.1080/08035250500539005 16801198.
Toiviainen-Salo, S., et al., 2008. Shwachman–Diamond syndrome is associated with structural brain alterations on MRI. Am. J. Med. Genet. A 146A (12), 1558–1564. http://dx.doi.org/10.1002/ajmg.a.3235418478597.
Vlooswijk, M.C., et al., 2010. Functional MRI in chronic epilepsy: associations with cognitive impairment. Lancet Neurol. 9 (10), 1018–1027. http://dx.doi.org/10.1016/S1474-4422(10)70180-020708970.
Wallace, G.L., Dankner, N., Kenworthy, L., Giedd, J.N., Martin, A., 2010. Age-related temporal and parietal cortical thinning in autism spectrum disorders. Brain 133 (12), 3745–3754. http://dx.doi.org/10.1093/brain/awq27920926367.
Wechsler, D., 1981. Wechsler Adult Intelligence Scale—Revised. The Psychological Corporation, San Antonio.
Wechsler, D., 1991. Wechsler Intelligence Scale for Children third edition. The Psychological Corporation, San Antonio.
Winkler, A.M., et al., 2010. Cortical thickness or grey matter volume? The importance of selecting the phenotype for imaging genetics studies. Neuroimage 53 (3), 1135–1146. http://dx.doi.org/10.1016/j.neuroimage.2009.12.02820006715.
Wozniak, J.R., Mueller, B.A., Ward, E.E., Lim, K.O., Day, J.W., 2011. White matter abnormalities and neurocognitive correlates in children and adolescents with myotonic dystrophy type 1: a diffusion tensor imaging study. Neuromuscul. Disord. 21 (2), 89–96. http://dx.doi.org/10.1016/j.nmd.2010.11.01321169018.
Zhang, S., Shi, M., Hui, C.C., Rommens, J.M., 2006. Loss of the mouse ortholog of the Shwachman–Diamond syndrome gene (SBDS) results in early embryonic lethality. Mol. Cell. Biol. 26 (17), 6656–6663. http://dx.doi.org/10.1128/MCB.00091-0616914746.